Enhanced transmission of TE polarized light through wire gratings

Hans Lochbihler
Louisenthal GmbH, Postfach 1185, 83701 Gmund am Tegernsee, Germany
(Received 21 April 2009; revised manuscript received 3 June 2009; published 24 June 2009)

Wire gratings exhibit enhanced transmission for TE polarized light, when its wavelength is approximately equal to the double of the spacing width. The enhanced transmission is caused by a resonance of the electromagnetic fields between the wires. The resonance in transmission has been studied for various wire profiles and grating materials, respectively. This different type of resonance practically does not have any dispersion. The wavelength of its maximum only changes slightly, when the angle of incidence is varied. The properties of this resonance are explained by a simple physical model. The enhanced transmission has been confirmed by measurements on gold-wire gratings having periods of 1000 and 500 nm, respectively. The absence of dispersion can be even observed by the naked eye on gratings with periods of 500 nm.

DOI: 10.1103/PhysRevB.79.245427 PACS number(s): 42.70.Qs, 73.20.Mf, 42.79.Dj, 74.25.Nf

I. INTRODUCTION

Wire gratings are nonadjacent one-dimensional periodic structures consisting of a conducting material, whereas the spacings between the wires are filled by a dielectric material or by air. Gratings having wires with a rectangular cross section are sometimes denoted as slit gratings in the literature. This kind of structure can be freestanding, lying on a substrate, or embedded in a dielectric. The diffraction of wire gratings in the resonance domain has been studied for many years.[1–22] In the beginning of the 1990s, resonances of TM polarized light (*E* vector of incident light perpendicular to the wires) were discovered on gold-wire gratings.[3] It was experimentally as well as numerically shown that these kinds of resonances can yield to almost 100% transmission of the incident light for highly conducting grating wires.[5] The enhanced light transmission is still present for gratings with very narrow slits.[11,20]

Later, a rather different feature was found for wire gratings: the excitation of surface-plasmon polaritons (SPs) by illuminating a wire grating with TM polarized light.[6] At that time, the excitation of SPs was only known for adjacent metallic surfaces.[23] SPs on wire gratings result in a strong field enhancement on the wire surface.[7] They travel along the grating surface and are damped by the finite conductivity of the metal that yields to strong absorption of the incident light. These absorption peaks can be measured directly, e.g., by means of a photoacoustic cell.[6] The fraction of "missing light" causes dips in the transmittance and reflectance spectra, respectively. Hence, SPs also can be verified more easily measuring transmittance and reflectance spectra, respectively. These kinds of measurements can be performed by means of commercial spectrophotometers. Finally, the dispersion of SPs is evaluated by locating the dips in the intensity spectra.

Inspired by the discovery of the extraordinary transmission through subwavelength hole arrays,[24] many researchers began to study transmittance properties of wire gratings for a large variety of profiles and materials.[9–21] All of these authors focused their studies on gratings illuminated by TM polarized light. Apart from the phase resonances in compound-wire gratings,[21] no fundamental new type of resonances were discovered for this case of polarization. Porto *et al.*[10] reported about transmission resonances for gratings with narrow slits. Unfortunately, these authors misleadingly explained the transmission process by the excitation of SPs. The enhanced transmission on gratings with narrow slits, however, describes the same physical issue as those resonances previously found by Lochbihler *et al.*[3,5] on wire gratings.

In this paper, however, I will present a rather different feature of wire gratings: the enhanced transmission of *TE polarized light* for wavelengths approximately equal to the grating period. In this case, the *E* vector of incident light oscillates *parallel* to the wires. Therefore, it is expected that this kind of resonance will behave rather different from those resonances in TM polarization. Hitherto, only a few papers presented transmittance data of wire gratings for TE polarization.[5,22] Lochbihler and Depine[5] outlined in their paper measured transmittance data as well as numerically calculated data at normal incidence for freestanding gold-wire gratings having various wire profiles. Moreno *et al.*[22] studied the transmittance numerically for a perfectly conducting wire grating lying on a dielectric substrate. They found peaks in transmission and explained them by coupling via surface modes.

The paper is organized as follows: first, I will present numerical transmittance data as well as the power losses for metallic wire gratings in the visible wavelength range. The angle of incidence and the wire cross section will be varied. Furthermore, the electromagnetic near fields of the resonance are shown for one example of a wire grating. Then, a simple physical model is derived from the electromagnetic formalism, which explains the relevant properties of the resonance. The numerical results are confirmed by measured transmittance data from gold-wire gratings. In Sec. IV, the behavior of this resonance is compared those resonances in TM polarization. Finally, applications for this kind of resonance are addressed.

II. NUMERICAL STUDY

A. Transmission and power losses

In this section, a rigorous modal method[25,26] is used for calculating the diffracted intensities of a plane wave on a

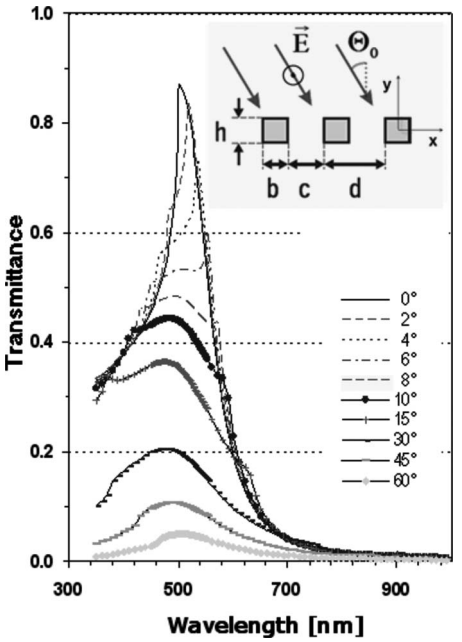

FIG. 1. Transmittance as a function of wavelength for an aluminum-wire grating ($d=500$ nm, $h=250$ nm, and $b=225$ nm) at various angles of incidence $\Theta_0=[0°,60°]$. The inset illustrates the geometry of the grating.

wire grating. For the sake of brevity, we concentrate our study mainly on metallic wire gratings having a rectangular cross section surrounded by vacuum. Later, some data are given for other grating structures, in order to show what happens when a wire grating deviates from this simple configuration. Let us first denote the main parameters that are varied in this numerical study. A plane wave with wavelength λ impinges on a wire grating forming an angle Θ_0 to the normal to the grating plane as shown in the inset of Fig. 1. Furthermore, the k vector of the plane of incidence is perpendicular to the grating wires (classical mounting). The E vector vibrates *parallel* to the wires. The grating is characterized by the period d, wire width b, the spacing c, and wire height h. In the numerical calculation, the data for the complex refractive indices of the metallic wires are used from Ref. 27.

The transmittance of an aluminum wire grating with a period $d=500$ nm, wire width $b=225$ nm, and a wire height $h=250$ nm in the visible wavelength range is shown in Fig. 1. The grating wires are surrounded by air. The angle of incidence Θ_0 is varied from normal incidence up to 60°. For normal incidence, almost 90% of the incident light is transmitted for $\lambda=d$. This wavelength coincides with the Rayleigh or Wood anomaly, where higher diffraction orders become evanescent. Tilting the grating slightly, the sharp transmission peak moves toward longer wavelengths obeying the dispersion of the Rayleigh anomaly

$$\lambda = d/n(1 \pm \sin \Theta_0), \tag{1}$$

where n represents the order of the evanescent wave.

For angles of incidence greater than approximately 5°, however, a second peak can be distinguished. This peak has its maximum at ≈500 nm and becomes more dominate for increasing the angle of incidence, while the peak from the Rayleigh anomaly vanishes. In contrast to the well-known resonances in TM polarization, this type of resonance obviously does not exhibit any dispersion.

Let us now consider the influence of the wire profile parameters to the resonance. Figure 2 shows the transmittance as well as the power losses as a function of wavelength at

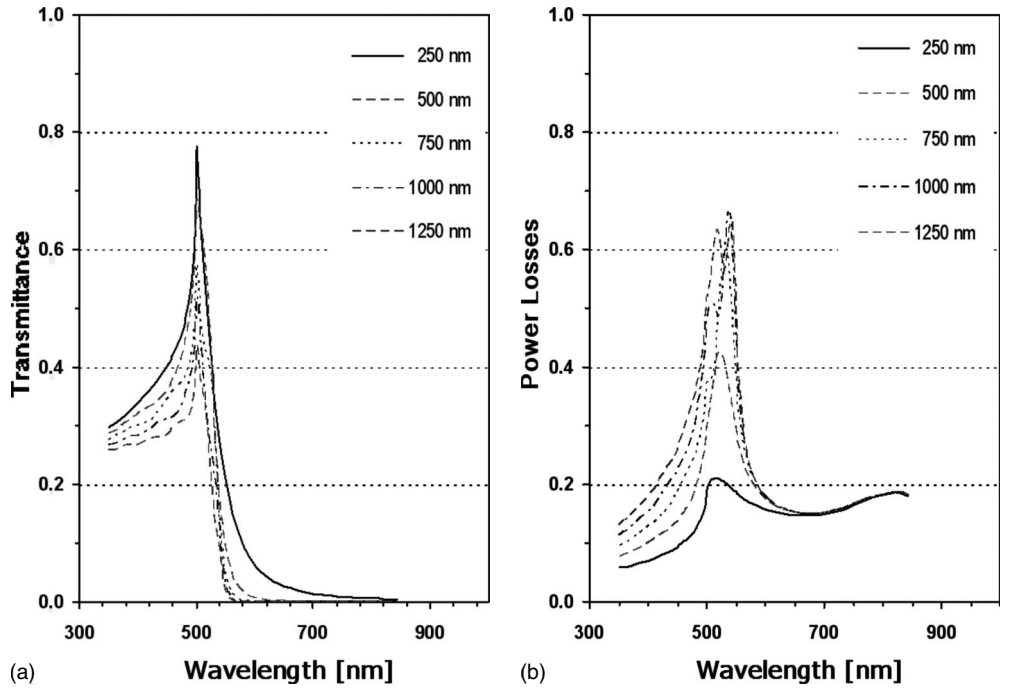

FIG. 2. (a) Transmittance and (b) power losses as a function of wavelength at normal incidence for an aluminum-wire grating ($d=500$ nm, $b=250$ nm) having various wire heights.

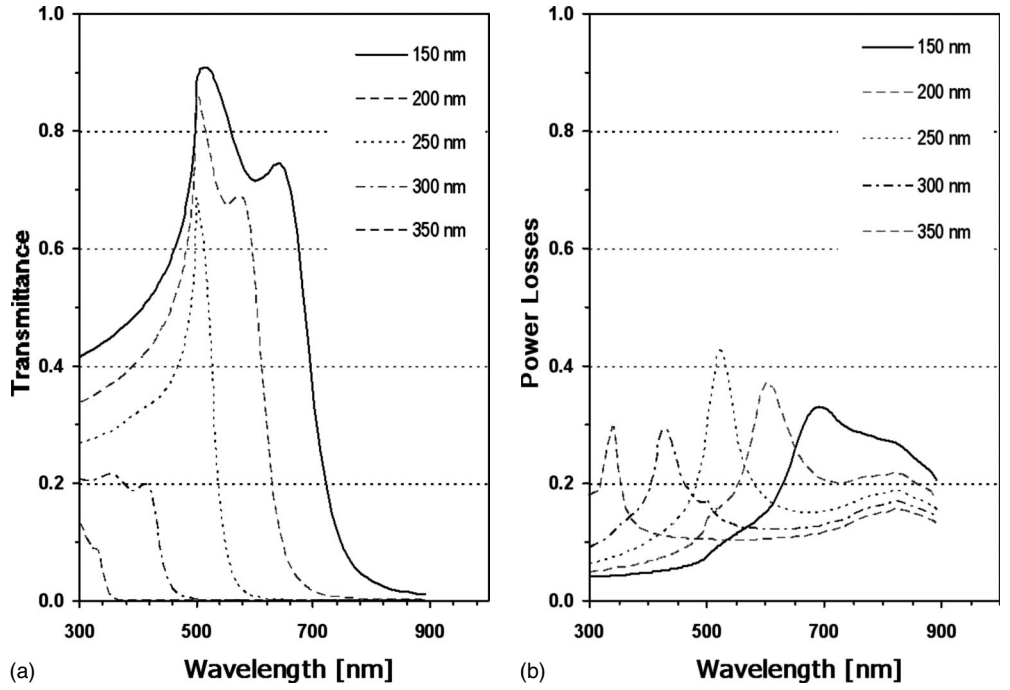

FIG. 3. (a) Transmittance and (b) power losses as a function of wavelength at normal incidence for an aluminum-wire grating (d =500 nm, h=500 nm) having various wire widths.

normal incidence for wire gratings having various wire heights h from 250 to 1250 nm. The remaining grating parameters are constant, identical to those of Fig. 1. The transmittance has its maximum at λ=500 nm for all wire heights; the maximum of power losses increases and moves slightly from 514 to 540 nm for increasing heights.

How does the resonance behave if the wire width is changed? For that, the wire width b is varied from 150 to 350 nm for an aluminum-wire grating with 500 nm period and a wire height of 500 nm. The numerical data for the transmittance and the power losses, respectively, are presented in Fig. 3. Increasing the wire width, the peak of power losses is shifted toward shorter wavelengths. While the grating with a wire width b=150 nm has its maximum at 692 nm, the resonance maximum for a grating with b=350 nm lies at 338 nm. The transmittance peak becomes sharper and is shifted in the same manner as the maximum of absorption. It is remarkable that the grating with b=150 nm exhibits a transmission maximum of about 90% in the subwavelength range.

Furthermore, the behavior of the resonance has been investigated for various grating materials. Some examples of transmittance data are illustrated in Fig. 4: (a) for a gold grating and (b) for a silver grating. Apart from the wire material, all remaining parameters of these gratings are identical to those from Fig. 3. A comparison between these figures demonstrates that the relationship between the wire width and the position of the transmittance maximum also holds for different kinds of grating materials. The full width at half maximum of the resonance, however, is influenced by the optical properties of the wires. Moreover, the transmittance maximum depends on the conductivity of the metallic wires. The highest transmittance can be achieved by a silver grating, the material with the highest conductivity in the visible wavelength range.

Do these bandpass characteristics also exist for wire gratings embedded in a dielectric? An answer to this question will be rather valuable given that embedded wire gratings are so well suited for cheap mass production in so many different technical applications.[8,28] For that, the transmittance of an aluminum grating embedded in a dielectric with refractive index n=1.5 such as plastics is exemplified in Fig. 5. Here, the grating period is 300 nm and the wire height is 200 nm. Similar as in Fig. 3, the transmittance has been calculated for various wire heights. Comparing these figures we can conclude that embedded wire gratings also exhibit strong resonances that are comparable to those of freestanding wire gratings. The bandpass characteristics of the resonance are shifted by a factor n toward longer wavelengths. This shift, however, could be compensated in the design of a grating by scaling down the geometrical parameters, i.e., the grating period and wire profile.

Finally, gratings having many other geometries of wire profiles have been investigated. It was found that the resonance phenomenon is still present if the wire profile deviates from a rectangular shape. But, the resonance becomes weaker for increasing asymmetric profile such as trapezoids. Rounded profiles, however, can exhibit a similar strength of the resonance as rectangular profiles. Detailed data will be published elsewhere.

B. Electromagnetic near fields

We know from the resonances on TM polarization that the electromagnetic fields are strongly enhanced in the vicinity of wires.[7,10] But, how do electromagnetic fields behave for the here presented resonance in TE polarization? For that, the electromagnetic near fields have been studied in the resonance maxima λ_{res}. Figure 6(a) shows the electric field $|E_z|^2$

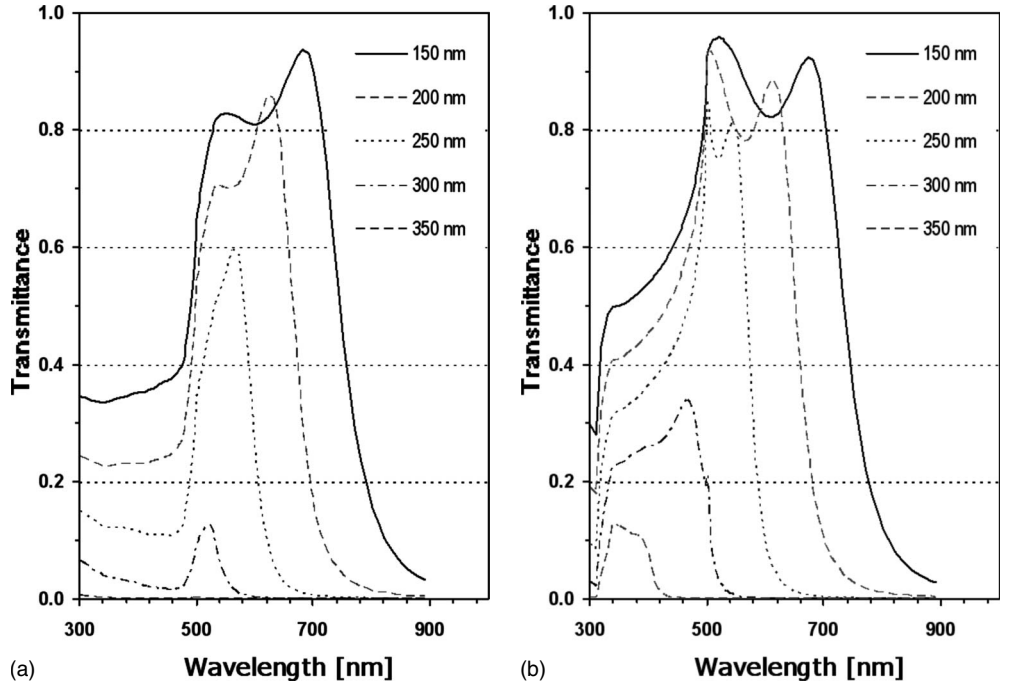

FIG. 4. Transmittance as a function of wavelength at normal incidence for a wire grating (d=500 nm, h=500 nm) having various wire widths for (a) gold wires and (b) silver wires.

normalized to the incident light for one period of an aluminum grating with parameters d=500 nm, b=250 nm, and h=500 nm at normal incidence. The resonance wavelength is λ_{res}=522 nm for which 42.6% of the incident light is absorbed (see also Fig. 3). The electric field is clearly enhanced in the spacings between the wires having a maximum of 13.3. The enhancement on the upper as well as on the lower wire surface is obviously poor. The magnetic field has its maximum intensity along the wire walls. The real part of the magnetic-field vector $H(x,y)$ is presented in Fig. 6(b), wherein the length of the arrows illustrates the logarithm to the basis (10) of the local field strength normalized to the incident light. Apparently, resonant curls of the magnetic field occur in the center of the spacings.

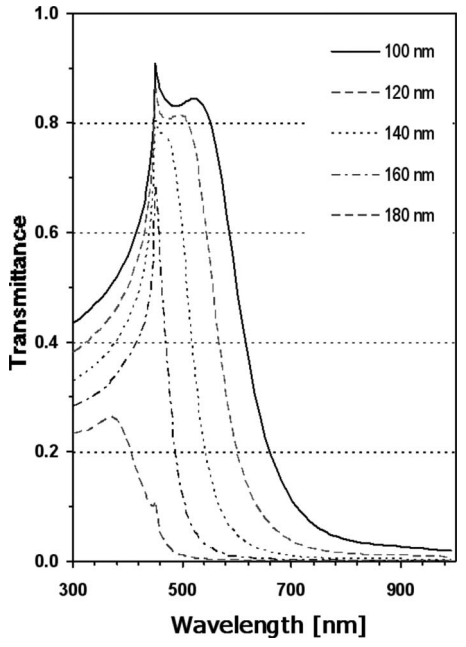

FIG. 5. Transmittance as a function of wavelength at normal incidence for an aluminum grating (d=300 nm, h=200 nm) embedded in a dielectric with n=1.5 having various wire widths.

We consider now the energy flow in the vicinity of wires for that resonant wavelength λ_{res}. The Poynting vector normalized to the incident radiation is defined by

$$\vec{S} = \Re[\vec{E} \times \vec{H}^*]. \tag{2}$$

Figure 6(c) shows $\vec{S}(x,y)$ in the vicinity of two grating periods. Again, the length of the arrows represents the logarithm of the strength of the local energy flux normalized to the incident power. This flow diagram demonstrates phenomenologically how the light transmits through the grating. The light behaves like a fluid and "flows" around the wires having its maximum intensity in the center between the spacings. The light absorption mainly occurs on the wire walls, since the light is "squeezed" to the metallic walls and consequently absorbed. This coupling mechanism is rather different from the observations of Moreno *et al.*[22] who studied the near fields of very thin gratings in TE polarization. They explained the enhanced transmission by the excitation of surface modes. Furthermore, they assumed in their model that the wires are perfectly conducting, an assumption not valid for the actual study. The transmission process for cavity resonances in TM polarization,[16] however, appears similar to the here discussed resonances in TE polarization.

Finally, the near fields for resonances also have been studied for non-normal incidence. For example, if the grating from Fig. 6 is tilted by 30°, the resonance maximum is shifted slightly from 522 to 516 nm, whereas the light ab-

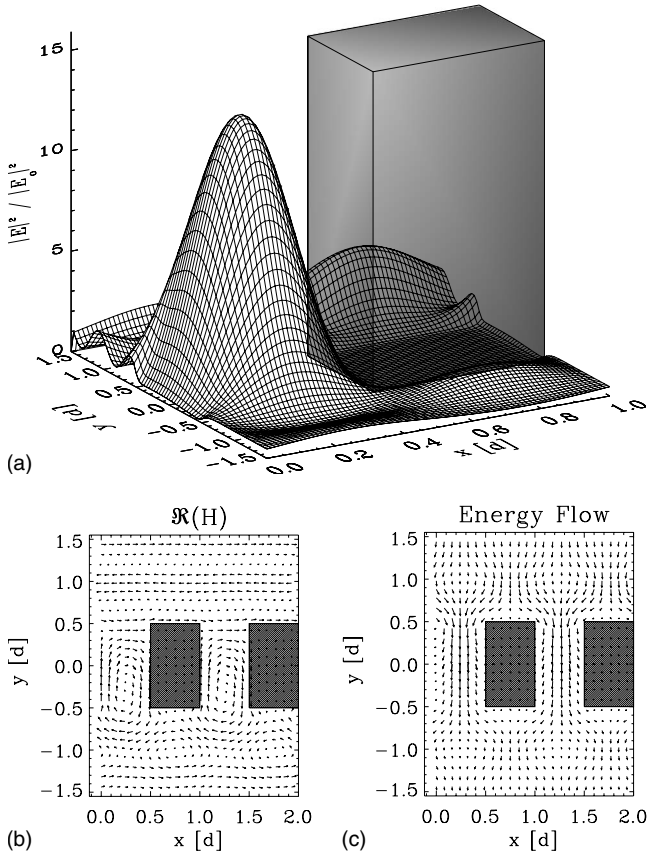

FIG. 6. Near fields for an aluminum-wire grating (d=500 nm, h=500 nm, and b=250 nm) in the resonance maximum λ_{res} =522 nm at normal incidence: (a) normalized squared E field, (b) real part of H field, and (c) Poynting vector.

sorption is reduced to 22.5% for this wavelength. As expected from the previous results, the near-field pattern does not change significantly for non-normal incidence. The field enhancement as well as the power losses, however, becomes poorer for increasing the angle of incidence.

C. Physical model for TE resonances

Unfortunately, the mathematical formalism of rigorous electromagnetic methods does not lend itself easily for an understanding of the physical origin of these resonances. Therefore, we will now simplify that exact mathematical formalism to the relevant parameters which are responsible for the resonant interaction of light with the wire grating.

In a first step, we only consider the zero-order coupling of the field amplitudes with the fundamental eigenmode of the modal field expansion within the grating region. It can be shown by numerical calculations that this resonance can be already well estimated by this single-mode approximation. The pattern of the near fields neglecting the higher order terms remains practically the same as in Fig. 6. In a further simplification we will use the surface impedance as a boundary condition on the metallic-wire surface avoiding the calculation of the electromagnetic fields inside the wires. The surface impedance boundary condition (SIBC) is given by the relation between the tangential components of the electric and magnetic fields at the boundary of a metal-vacuum interface

$$\vec{E}_{\parallel} = Z\hat{n} \times \vec{H}_{\parallel}, \tag{3}$$

wherein Z is the surface impedance and $\hat{n}$ denotes a normal unit vector on the boundary pointing into the free space side.

It was shown in Refs. 4–6 that the approximation of a constant impedance $Z=1/\sqrt{\epsilon}$ (ϵ denotes the permittivity of the metal) already yields almost the same results for metallic-wire gratings in the near infrared as rigorous methods. Finally, it was found that the SIBC method still predicts these resonances of TE polarized light very well even in the visible wavelength range. This is quite astonishing and can be understood by taking a look at the near fields from Fig. 6: the electromagnetic fields only enter very slightly into the wires and the strength of the electric field is low on the wire surface. Therefore, the resonances can be calculated quite accurately by means of the SIBC method even for the case of "fair conducting metals." Moreover, the SIBC method was already successfully applied by many other authors for explaining resonances on slit gratings.[10,14,16,17]

Using the formalism from Ref. 4, the zero-order transmittance I_0^T can be estimated from the first term of the modal field expansion, and we obtain

$$I_0^T = |T_0|^2 \approx |[J_{0,0}](a_0 - b_0)|^2, \tag{4}$$

with the field amplitudes a_0 and b_0 given by

$$a_0 \approx \frac{\delta[J_{0,0}]^{-1}}{i\mu_0 \cot(\mu_0 h/2) + \delta}, \tag{5}$$

$$b_0 \approx \frac{\delta[J_{0,0}]^{-1}}{-i\mu_0 \tan(\mu_0 h/2) + \delta}, \tag{6}$$

whereas $\delta = k_0 \cos\Theta_0[K_{0,0}][J_{0,0}]$, $\mu_0 = \sqrt{(k_0^2 - \beta_0^2)}$, and $k_0 = 2\pi/\lambda$. For the definition of the matrices $[K_{n,m}]$ and $[J_{n,m}]$, the reader is referred to Ref. 4. The complex zero β_0 is the first eigenvalue from the transcendental equation

$$\tan(\beta_m c) = \frac{2\eta\beta_m}{(\eta\beta_m)^2 - 1}, \tag{7}$$

with $\eta = Zi/k_0$. Subsequently, Eq. (4) can be simplified to

$$I_0^T \approx \left| \frac{2i\mu_0/\sin(\mu_0 h)}{\mu_0^2 + \delta^2 + 2i\delta\mu_0 \cot(\mu_0 h)} \right|^2. \tag{8}$$

It can be shown very easily that the resonance is mainly formed by the term $\mu_0/\sin(\mu_0 h)$. Finally, the wavelength of the resonance maximum λ_{res} can be estimated by

$$\lambda_{res} \approx 2\pi/\beta_0 \approx \frac{2c}{1 - 2\eta/c}. \tag{9}$$

From this simple relation, we can deduce immediately all properties which we have previously found in the numerical study:

(i) The resonance wavelength λ_{res} is approximately equal to the double of the wire spacings: $\lambda_{res} \approx 2c$. The peak in the wavelength spectrum is slightly shifted away from the value

$2c$ caused by the finite conductivity of the grating material.

(ii) A variation in angle of incidence does not change the position of the resonance maximum since the eigenvalue Eq. (7) does not depend on Θ_0.

(iii) The position of the resonance maximum is not influenced by the wire height h since Eq. (7) does not depend on h.

The same properties for the resonance can be found if we consider the power losses. Again, we use the SIBC method to calculate the light absorption on the grating. For this case, the SIBC method has a further advantage: it may show us very easily the local absorption along the wire surface. Therefore, it can be demonstrated that the resonant light absorption occurs mainly on the wire walls, i.e., on the surface between the wires. This coincides with the fact that the strength of the magnetic field is the highest on the wire walls. The term for the power losses on the walls is given by

$$P_{\text{walls}} = \frac{4\Re Z}{\Im(\beta_0^2)k_0^2 \cos\Theta_0}\{\Im[\mu_0 \cot(\mu_0 h/2)]|a_0|^2 - \Im[\mu_0 \tan(\mu_0 h/2)]|b_0|^2\}. \quad (10)$$

Equation (10) can be simplified in an analogous manner as the expression for the transmittance in Eq. (4). Finally, we obtain a similar relationship for the wavelength of the maximum light absorption. This proves that the enhanced transmission simultaneously causes a peak in the power losses.

III. EXPERIMENTAL RESULTS

The experiments have been performed on freestanding gold-wire gratings, each having a diameter of approximately 15 mm. For details of grating manufacturing and characterization of the grating parameters, the reader is referred to the literature.[3] The investigated gratings have a period of 991.2 and 500 nm, respectively. The transmission measurements have been performed by means of a spectrophotometer with narrowed beam angles and Glan prisms as polarizers. The averaged divergence of the incident beam was below 0.5°. The gratings could be tilted in the sample compartment very accurately by stepper motors.

Figure 7 shows the measured transmittance for a wire grating with a period of 991.2 nm for various angles of incidence. The wire profile is nearly rectangular. It can be characterized by a trapezoid yielding the quantities $h=367$ nm, $b=467$ nm, and the angle of its sides $s=88°$ ($s=90°$ denotes a rectangular shape).

These measured data are then compared with the calculated transmittance in the same figure. In the calculation, for sake of simplification, a rectangular wire profile with $h=370$ nm and $b=470$ nm was assumed. The theory agrees very well with the experimental data, only the curves for $\Theta_0=0°$ and 15° deviate somewhat in the wavelength region between 550 and 900 nm. These variations, however, are caused by slight deviations of real wire profile from the assumed rectangular shape.

Figures 8(a) and 8(b) show measured transmittance data for two other gold-wire gratings with nearly rectangular wire profile but rather different wire widths: $b=433$ nm and $b=512$ nm, whereas the wire height is approximately identical. The transmittance curves confirm the findings from the numerical study: the resonance wavelength depends on the wire width and is shifted toward shorter wavelengths for increasing wire widths. But, keep in mind that the peaks for near normal incidence are dominated by the Rayleigh anomaly. The peak difference between the resonances of these two gratings is about 150 nm, which agrees well with the estimation using relation (9).

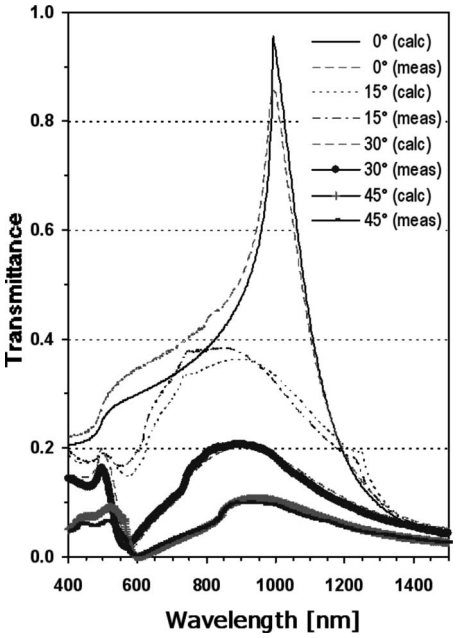

FIG. 7. Comparison of measured and calculated transmittances as a function of wavelength at various angles of incidence $\Theta_0=[0°,45°]$ for a gold-wire grating with parameters $d=991.2$ nm, $h=367$ nm, $b=467$ nm, and $s=88°$. For the calculation, a rectangular wire profile with $h=370$ nm and $b=470$ nm was assumed.

Furthermore, the resonance wavelength is only slightly moved for both gratings, when the angle of incidence is varied. Hence, the absence of dispersion is in agreement with the theoretical considerations from Chapter II.

Finally, the transmittance of a gold-wire grating with a period of $d=500$ nm was measured in the visible wavelength range. For this grating, however, the wire profile deviates somewhat more from a rectangle as the grating discussed above. It can be roughly characterized by a rectangle with the parameters $h=280$ nm and $b=300$ nm. The transmittance curves for angles of incidence Θ_0 between 0° and 45° are shown in Fig. 9. The overall transmittance is lower compared to the other gratings from Fig. 8 due to the smaller spacings. The resonance maximum lies approximately at 530 nm. Again, this grating does not exhibit any dispersion for this resonance.

A very impressive experiment is to observe the transmitted light through this grating directly by the naked eye. For that, I took a polarizer and placed it in front of a light source, e.g., daylight. Then, I orientated the grating from Fig. 9 in front of the polarizer such that the geometry of incident light forms the fundamental cases of polarization. In case of TE polarization, the grating appears green at normal incidence.

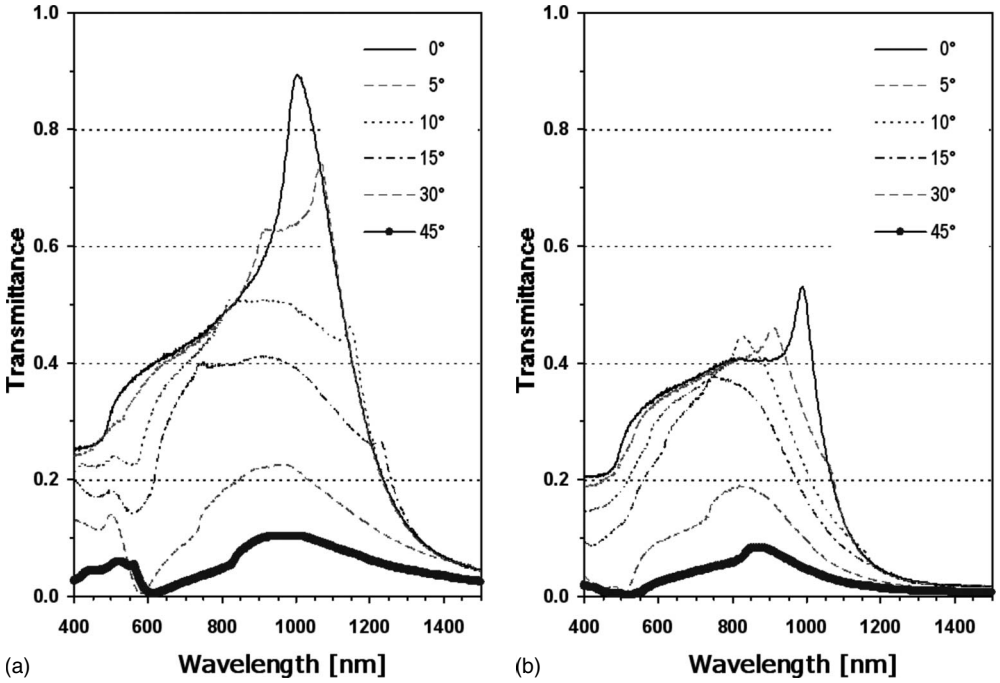

FIG. 8. Measured transmittance as a function of wavelength at various angles of incidence $\Theta_0=[0°,45°]$ for gold-wire gratings with parameters: (a) $d=991.2$ nm, $h=477$ nm, $b=433$ nm, and $s=84°$ and (b) $d=991.2$ nm, $h=482$ nm, $b=512$ nm, and $s=87°$.

The color does not change when the grating is turned by the angle Θ_0 from 0° up to 45°. For the case of TM polarization, however, the transmitted color is blue at normal incidence. When the grating is only slightly tilted by about 15°, the grating changes its color rapidly from blue to yellow. Then, it becomes red for larger angles of incidence. These colors also were correctly predicted by numerical calculations using the emissivity spectrum of a standard light source *D*65 which represents the daylight spectrum and the spectral sensitivity function of the human eye. A detailed explanation for the numerical evaluation of colors can be found in textbooks.[29]

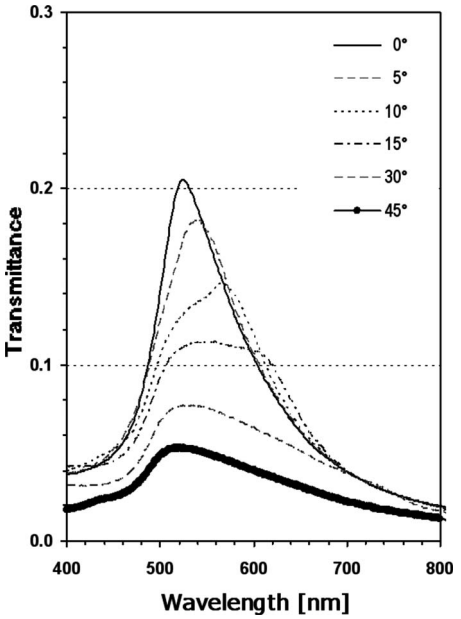

FIG. 9. Measured transmittance as a function of wavelength at various angles of incidence $\Theta_0=[0°,45°]$ for a gold-wire grating with a period of 500 nm and a wire profile that can be roughly characterized by a rectangle with $h=280$ nm and $b=300$ nm.

This experiment proves in a simple manner the absence of dispersion for the here discussed resonance in TE polarization. In contrast, light transmission in TM polarization is dominated by the cavity resonances. Its well-known dispersion[9,10,18] shifts the color from blue to red for increasing angles of incidence.

IV. DISCUSSION

It would be interesting to study colors of transmitted light for gratings having parameters like those in figures of chapter II. It is expected that these gratings exhibit an even stronger color effect than the grating of Fig. 9. Exploiting resonances in TE polarization, wire gratings can be used as efficient light filters. Furthermore, light radiating at various angles, e.g., diffuse light or focused light beams, can be filtered efficiently by wire gratings, since the resonance wavelength does not depend on the angle of incidence.

In principle, the transmission maximum can be tuned for a wide range of wavelengths by varying the spacings between the wires. But, it was found that the plane wave couples most strongly to the zeroth mode for $\lambda \approx d$ for which the spacings are $c \approx d/2$.

It is worth to mention that also higher order coupling exists for this kind of resonance. Figures 7 and 8 show peaks at about 500 nm which result from resonant first-order coupling. The transmission peaks are much smaller as the peaks for the zeroth order coupling, since the higher mode coupling is less efficient than the zeroth mode coupling.

The physical origin of this kind of resonance is rather different from the excitation of SPs for TM polarization. SPs

are not excited on metallic wire gratings at normal incidence in the first-order coupling mode.[6] In contrast, resonances in TE polarization are still present for normal incidence. Moreover, they do not cause a strong energy flow along the grating plane as SPs do. The enhancement of electromagnetic fields in the vicinity of the wires is generally lower than for SPs. Hence, these resonances do not exhibit properties of quasiparticles and cannot be attributed to SPs. Clearly, no momentum can be transferred from an impinging photon at normal incidence to a quasiparticle propagating along the grating plane.

Resonances in TE polarization, however, have similarities with those cavity resonances in TM polarization, although the electromagnetic fields are interchanged in orientation. A comparison of both types of resonances shows that the energy flow and the near-field distribution between the wires appear similar. In both cases of resonance, the cavities between the wires act as resonators. While the wire height forms the resonator length for the resonances in TM polarization (like in a Fabry-Perot interferometer), the spacing between the wires represents the resonator length for resonances in TE polarization.

V. CONCLUSIONS

A different type of resonance was presented that occurs on wire gratings in TE polarization. These resonances cause significant peaks in transmittance and simultaneous peaks in absorption. Strongest resonance effects were observed for zero-mode coupling and for wire spacings approximately equal to wire widths. Hence, resonance maxima appear for wavelengths approximately equal to the grating period. In contrast to the well-known resonances in TM polarization and the Rayleigh anomaly, these resonances do not exhibit any dispersion.

The transmittance and the power losses were studied by means of a rigorous modal method for various wire profiles and grating materials, respectively. The influence of the grating parameters to the resonance as well as the absence of dispersion could be explained by a simple physical model derived from a surface impedance method. The approximated surface impedance method predicted the resonances in TE polarization quite accurately even in the visible wavelength range and provided physical insight into the behavior of the resonances.

The numerical data were confirmed by transmittance measurements on freestanding gold-wire gratings. One of these gratings transmits approximately 90% of the incident light in the resonance maximum. Another gold-wire grating having a period of 500 nm exhibited interesting color features arising from resonant transmission. For this grating, the absence of dispersion in TE polarization could be observed even by the naked eye. This effect has very promising applications in color filtering.

ACKNOWLEDGMENT

I thank Peter Predehl (Max-Planck-Institut für Extraterrestrische Physik, Garching) for using his measurement facilities.

[1] A. A. Volkov, B. P. Gorshunov, A. A. Irisov, G. V. Kozlov, and S. P. Lebedev, Int. J. Infrared Millim. Waves **3**, 19 (1982).
[2] J. Y. Suratteau and R. Petit, Int. J. Infrared Millim. Waves **6**, 831 (1985).
[3] H. Lochbihler and P. Predehl, Appl. Opt. **31**, 964 (1992).
[4] H. Lochbihler and R. A. Depine, Appl. Opt. **32**, 3459 (1993).
[5] H. Lochbihler and R. A. Depine, Opt. Commun. **100**, 231 (1993).
[6] H. Lochbihler, Phys. Rev. B **50**, 4795 (1994); **53**, 10289 (1996).
[7] H. Lochbihler, Opt. Commun. **111**, 417 (1994).
[8] H. Tamada, T. Doumuki, T. Yamaguchi, and S. Matsumoto, Opt. Lett. **22**, 419 (1997).
[9] U. Schröter and D. Heitmann, Phys. Rev. B **58**, 15419 (1998).
[10] J. A. Porto, F. J. Garcia-Vidal, and J. B. Pendry, Phys. Rev. Lett. **83**, 2845 (1999).
[11] S. Astilean, Ph. Lalanne, and M. Palamaru, Opt. Commun. **175**, 265 (2000).
[12] J. P. Kottmann, O. J. F. Martin, D. R. Smith, and S. Schultz, Phys. Rev. B **64**, 235402 (2001).
[13] A. Barbara, P. Quemerais, E. Bustarret, and T. Lopez-Rios, Phys. Rev. B **66**, 161403(R) (2002).
[14] J. M. Steele, C. E. Moran, A. Lee, C. M. Aguirre, and N. J. Halas, Phys. Rev. B **68**, 205103 (2003).
[15] S. Collin, F. Pardo, R. Teissier, and J. L. Pelouard, Phys. Rev. B **63**, 033107 (2001).
[16] F. J. Garcia-Vidal and L. Martin-Moreno, Phys. Rev. B **66**, 155412 (2002).
[17] K. G. Lee and Q-Han Park, Phys. Rev. Lett. **95**, 103902 (2005).
[18] Y. Pang, C. Genet, and T. W. Ebbesen, Opt. Commun. **280**, 10 (2007).
[19] E. Popov, M. Neviere, S. Enoch, and R. Reinisch, Phys. Rev. B **62**, 16100 (2000).
[20] M. M. J. Treacy, Phys. Rev. B **66**, 195105 (2002).
[21] D. C. Skigin and R. A. Depine, Phys. Rev. E **74**, 046606 (2006).
[22] E. Moreno, L. Martin-Moreno, and F. J. Garcia-Vidal, J. Opt. A, Pure Appl. Opt. **8**, S94 (2006).
[23] H. Räther, *Surface Plasmons on Smooth and Rough Surfaces and on Gratings* (Springer-Verlag, Berlin, 1988).
[24] T. W. Ebbesen, H. J. Lezec, H. F. Ghaemi, T. Thio, and P. A. Wolf, Nature (London) **391**, 667 (1998).
[25] L. C. Botten, M. S. Craig, R. C. McPhedran, J. L. Adams, and J. R. Andrewartha, Opt. Acta **28**, 1087 (1981); **28**, 1103 (1981).
[26] L. Li, J. Mod. Opt. **40**, 553 (1993); J. Opt. Soc. Am. A **10**, 2581 (1993).
[27] *Handbook of Optical Constants of Solids*, edited by E. D. Palik (Academic Press, Orlando, 1985).
[28] D. Wang, W. Liu, Q. Xiao, and J. Shi, Appl. Opt. **47**, 312 (2008); V. Auzelyte, H. H. Solak, Y. Ekinci, R. MacKenzie, J. Vörös, S. Olliges, and R. Spolenak, Microelectron. Eng. **85**, 1131 (2008).
[29] G. A. Klein, *Farbenphysik Für Industrielle Anwendungen* (Springer-Verlag, Berlin, 2004).